http://dx.doi.org/10.5012/bkcs.2012.33.7.2200

One-Dimensional Core/Shell Structured TiO_2/ZnO Heterojunction for Improved Photoelectrochemical Performance

In Ae Ji, Min-Joon Park,[†] Jin-Young Jung,[†] Mi Jin Choi, Yong-Woo Lee,[*] Jung-Ho Lee,[†,*] and Jin Ho Bang[*]

Department of Chemistry and Applied Chemistry and [†]Department of Chemical Engineering, Hanyang University, Ansan, Kyeonggi-do 426-791, Korea
[*]E-mail: jbang@hanyang.ac.kr (J. H. Bang), yongwoolee@hanyang.ac.kr (Y.-W. Lee), jungho@hanyang.ac.kr (J.-H. Lee)
Received February 21, 2012, Accepted March 28, 2012

One-dimensional TiO_2 array grown on optically transparent electrode holds a promise as a photoelectrode for photoelectrochemical water splitting; however, its crystal structure is rutile, imposing constraints on the potent use of this nanostructure. To address this issue, a heterojunction with type-II band alignment was fabricated using atomic layer deposition (ALD) technique. One-dimensional core/shell structured TiO_2/ZnO heterojunction was superior to TiO_2 in the photoelectrochemical water splitting because of better charge separation and more favorable Fermi level. The heterojunction also possesses better light scattering property, which turned out to be beneficial even for improving the photoelectrochemical performance of semiconductor-sensitized solar cell.

Key Words : TiO_2/ZnO heterojunction, Photoelectrochemical water splitting, Atomic layer deposition, Semiconductor-sensitized solar cell

Introduction

Solar energy has recently recaptured enormous interest as a future energy resource.[1] As part of efforts to utilize solar energy, the production of hydrogen gas (H_2) *via* photocatalysis has received scientists' tremendous attention as it holds great promise as an inexpensive, renewable, and environmentally benign energy carrier. The production of H_2, however, heavily relies on the steam-reforming of hydrocarbons (*e.g.*, natural gas or methane) at present, which is undesirable from the viewpoint of cost-efficiency and environmental impact of the process.[2] As a means of addressing such issues, direct water splitting using photocatalysts has long been investigated for the development of a low-cost, environmentally benign process for H_2 production.[3-7] The utilization of heterogeneous photocatalysts for water splitting was initiated by Honda and Fujishima in 1972,[8] and their pioneering work has led to extensive research on TiO_2, hoping for developing an efficient H_2 production system. A wide variety of strategies have been developed in order to enhance the photocatalytic activity of TiO_2. Fabricating nanostructures of TiO_2 – such as nanowires, nanotubes, nanoplates, or porous spheres – is a representative example among the sustained efforts.[9-12] Of the diverse TiO_2 nanostructures, one-dimensional nano-geometry has particularly received great attention due to its superior charge transport ability, which significantly suppresses the recombination of charge carriers.[13] In general, one-dimensional, vertically aligned TiO_2 has been fabricated by the electrochemical etching method where Ti foil is etched into columnar array in an electrolyte containing NH_4F under applied voltage.[14-16] The utilization of TiO_2 nanotubes, however, has been somewhat restricted because of non-transparency associated with Ti foil, the use of toxic electrolyte, and the need of multiple steps involved in the synthesis. To circumvent these constraints, we have recently developed a simple hydrothermal synthetic route, where single-crystalline TiO_2 nanorods grow directly on optically transparent electrode (OTE).[17] The TiO_2 nanorod photoelectrode was utilized in photoelectrochemical cells and proved to be superior to TiO_2 particulate counterpart in terms of electron transport.[17] Despite the successful demonstration of the TiO_2 nanorods as a photoanode, its catalytic activity in the photoelectrochemical water splitting is quite low mainly because the crystal structure of the TiO_2 nanorods is rutile.[17,18] While rutile-phase TiO_2 possesses smaller bandgap (3.0 eV) than anatase-phase TiO_2 (3.2 eV), the conduction band-edge of the rutile-phase TiO_2 is positioned in a more positive potential, which is located below the standard reduction potential of H^+/H_2 couple (0 V *vs*. normal hydrogen electrode).[19] This implies that the Fermi level of the rutile-phase TiO_2 is less favorable than that of anatase-phase counterpart for H_2 generation, thereby requiring much higher bias voltage (Note that Pt sustains H_2 production in the photoelectrochemical cells). As an approach to overcoming this restraint, we report hereby the fabrication of core/shell structured TiO_2/ZnO nanorod array *via* atomic layer deposition (ALD) technique. The newly developed TiO_2/ZnO heterojunction significantly improved its performance in the photoelectrochemical water splitting cell due to the beneficial synergetic effects of the heterostructured nanocomposite. Further, we demonstrated that the TiO_2/ZnO photoelectrode could be utilized as an oxide substrate for a semiconductor-sensitized solar cell to boost up its energy conversion efficiency.

Experimental

Synthesis of TiO_2 and TiO_2/ZnO Heterojunction Arrays. TiO_2 nanorod array on conducting glass electrodes was prepared by the hydrothermal method as reported previously.[17] Titanium (IV) butoxide (Aldrich 97%, 0.35 mL) was added dropwise into 6 M aqueous HCl solution (15 mL) under vigorous stirring. The stirring was continued for 30 min at room temperature. The solution was then transferred to a Teflon-lined stainless steel autoclave, and a piece of optically transparent electrode (OTE) cut from F-doped SnO_2 (FTO) glass (Pilkington TEC 15, Hartford Glass, Inc.) was immersed into the solution. The autoclave was sealed and placed in an oven at 150 °C for 4 h. After cooling the autoclave to room temperature, the TiO_2 nanorod film was washed several times with deionized water to remove adsorbed precursor species and dried under air. The TiO_2 nanorods were overcoated with ZnO by ALD (D-100, thermal ALD) at 200 °C with diethylzinc as a zinc precursor and water as an oxygen source. The pressure of the ALD chamber was maintained at 0.5 torr, and diethylzinc was kept at 10 °C and carried by nitrogen gas to the chamber. The average growth rate of ZnO was 1.8 Å/cycle, which were measured by TEM analysis, and the ALD cycles were repeated 100 times.

Preparation of CdSe-TiO_2 and CdSe-TiO_2/ZnO Photoelectrodes. Thin layers of CdSe were electrochemically deposited onto the TiO_2 and the TiO_2/ZnO heterojunction array films according to previous reports.[20,21] Galvanostatic deposition was performed at room temperature in an aqueous solution containing 0.05 M cadmium acetate dihydrate, 0.1 M sodium nitrilotriacetate, and 0.05 M sodium selenosulfite adjusted to pH ~9 using a two-electrode electrochemical cell with a Pt counter electrode. The total amount of charge passed during the deposition was 0.25 C/cm^2 for both TiO_2 and TiO_2/ZnO heterojunction array films. The resulting electrodes were rinsed with deionized water several times, dried under air, and annealed under air at 350 °C for 1 h to improve the crystallinity of CdSe. The photoelectrodes will hereafter be referred to as CdSe-TiO_2 and CdSe-TiO_2/ZnO, respectively.

Characterization. X-ray diffraction (XRD) patterns were recorded using an X-ray diffractometer (Rigaku D/Max-2500/PC). Scanning electron microscopy (SEM) was performed using a field-emission scanning electron microscope (Hitachi S-4800 FESEM) equipped with an EDS (energy dispersive X-ray spectroscopy) detector. Transmission electron microscopy (TEM) was carried out using a JEOL 2010F equipped at an acceleration voltage of 200 kV. Transmission and reflectance spectra were recorded using a Perkin Elmer spectrophotometer (Lambda 750).

Photoelectrochemical Measurements. Current-voltage (*I-V*) characteristics of the photoelectrodes were recorded using a potentiostat (CH Instruments, CHI 660D) at a scan rate of 50 mV/s in a three-electrode configuration using Pt gauze as a counter electrode and a saturated calomel electrode (SCE) as a reference. An aqueous NaOH solution (0.1 M) was used when measuring photocurrent with TiO_2 and TiO_2/ZnO electrodes, whereas an aqueous Na_2S solution (0.1 M), a widely used hole scavenger for CdSe, was employed for the photocurrent measurement of CdSe-TiO_2 and CdSe-TiO_2/ZnO electrodes because NaOH cannot prevent the photocorrosion of CdSe effectively. Prior to the measurement, N_2 gas was purged through the electrolytes for 30 min to ensure oxygen-free electrolytes. An Oriel 300 W xenon arc lamp equipped with Air Mass (AM) 1.5 filter (Oriel) served for a light source; for ultraviolet light (UV) irradiation, AM 1.5 filter was removed.

Results and Discussion

Coupling two semiconductor materials to construct heterojunction with a staggered band-edge alignment (*i.e.*, type-II band alignment) has been widely performed to improve the catalytic activity of photoelectrodes. To date, a variety of inorganic heterojunction architectures have been developed to enhance the efficiency of photoelectrochemical water splitting cell.[22-30] In our study, we adapted this long-established strategy to enhance the photocatalytic activity of hydrothermally grown TiO_2 nanorod array. As a coupling material, we chose ZnO because its conduction band-edge is positioned at more negative potential in comparison with that of TiO_2, thus being suitable for building the type-II band alignment (Scheme 1).[31] Note that while there has been concern on the photocorrosion of ZnO,[32] it has proven its photostability with a proper hole scavenger in many reports.[28-30,33-37]

TiO_2/ZnO heterojunction could be beneficial because the recombination of charge carriers can be significantly suppressed due to the spatial separation of electron-hole pairs. The improved photoelectrochemical activity due to the electron-hole separation in the TiO_2/ZnO heterojunction has been well-documented in previous reports.[28-30] This improved charge separation is also capable of raising the Fermi level of the TiO_2/ZnO heterojunction, rendering it more

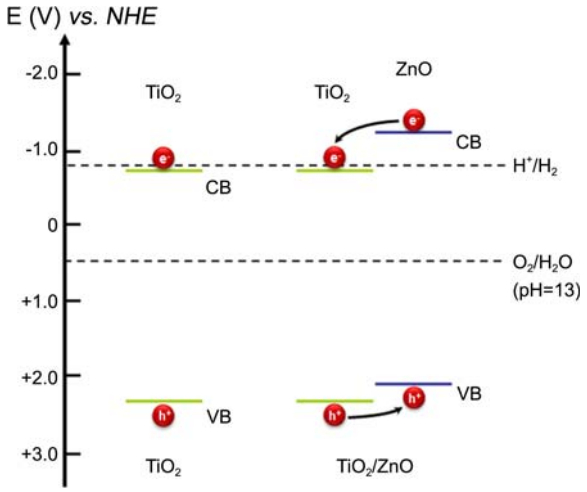

Scheme 1. Energy diagrams of TiO_2 and of TiO_2/ZnO heterojunction at pH of 13.

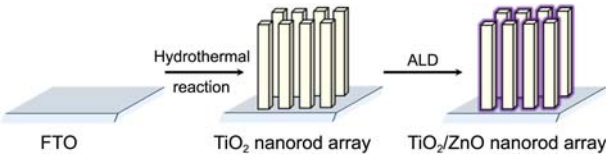

Scheme 2. Illustration of synthesis of core/shell structured TiO_2/ZnO heterojunction array on OTE.

favorable for H_2 evolution.[28] The preparation of TiO_2/ZnO heterojunction array, however, remains challenging in spite of well-developed wet chemistry of ZnO. A difficulty in the synthesis is associated with the highly hydrophobic surface of the hydrothermally grown TiO_2 nanorod array, which prevents any aqueous ZnO precursor solutions from penetrating into grooves along the nanorods.[38] This synthetic hurdle inhibits the conformal coating of ZnO over the TiO_2 nanorods, which can form one-dimensional, core/shell structured TiO_2/ZnO heterojunction. A very recent report describes the production of TiO_2/ZnO heterojunction; however, in this synthesis ZnO can grow only from the tips of the hydrothermally grown TiO_2 nanorods because of the poor wettability of its surface, yielding branched ZnO rods on top of the TiO_2 nanorods.[39] Despite some potent advantages of this intriguing nanostructure, the benefits obtained from the type-II band alignment would be greatly limited as the heterojunction in this nanostructure is formed only on a small portion of TiO_2 – the tips of the TiO_2 nanorods. In our approach, we employed ALD technique to attain uniform, conformal ZnO coating over the TiO_2 nanorod array, producing core/shell structured TiO_2/ZnO heterojunction array (Scheme 2). To the best of our knowledge, this is the first demonstration of conformal ZnO coating over rutile-phase, hydrophobic TiO_2 nanorod array. ALD emerges as a powerful technique for the deposition of thin films.[40] Not only does this technique achieve conformal coating over various substrates at relatively low temperatures, but it also allows for precise thickness control. In our synthesis, the ALD was performed using diethylzinc and water as a zinc and oxygen source, respectively. Alternating exposures to diethylzinc and water led to the growth of thin ZnO film over the TiO_2 nanorods.

XRD analysis in Figure 1 reveals the formation of ZnO on the surface of the TiO_2 nanorods *via* the ALD process. The diffraction peaks from the TiO_2 nanorods indicate that the hydrothermal reaction yields rutile-phase TiO_2 (JCPDS 21-1276). After the ALD process was carried out, the film was re-examined, and the XRD pattern displays additional peaks stemming from wurtzite-phase ZnO (JCPDS 36-1451). The diffraction peaks from the ZnO are broad and intense, implying that ZnO nanocrystallites were formed even at the low-temperature reaction. In addition, there are no other peaks except from TiO_2 and ZnO, revealing that the low-temperature ALD process inhibits the formation of other possible solids such as Zn_2TiO_4 and $ZnTiO_3$, which may be formed at high temperature reactions.[41]

The morphology of the TiO_2 and TiO_2/ZnO heterojunction

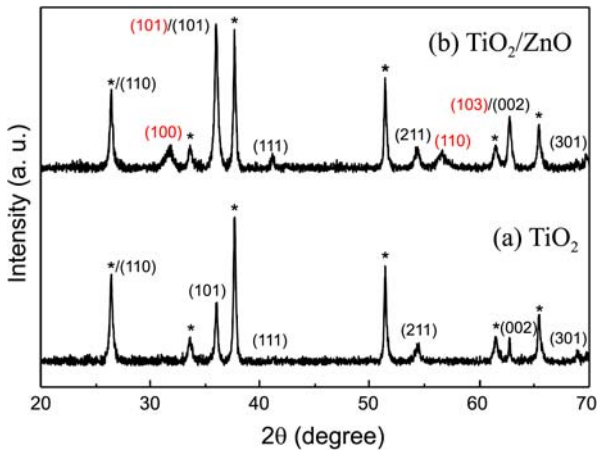

Figure 1. XRD patterns of (a) TiO_2 nanorod and (b) TiO_2/ZnO heterojunction array grown on FTO substrate (peaks from F-SnO_2 coated glass substrate are marked with asterisks and peaks from ZnO are labelled in red).

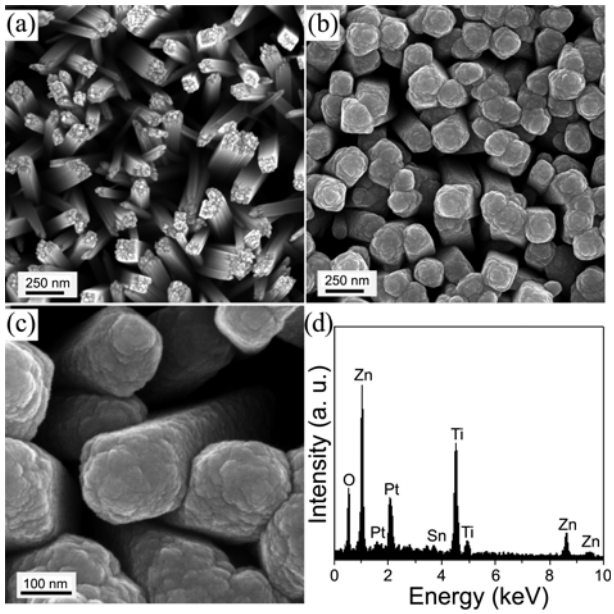

Figure 2. SEM images of (a) TiO_2 nanorod and (b and c) TiO_2/ZnO heterojunction array; (d) EDS analysis of TiO_2/ZnO heterojunction array (Pt signals are from Pt overcoating for SEM analysis).

array was examined using a scanning electron microscope. Figure 2(a) shows the SEM image of the TiO_2 nanorod array grown on FTO substrate. The TiO_2 nanorods were typically 90-100 nm wide and ~2 μm long, as consistent with our previous report.[17] Figure 2(b) and (c) displays the SEM images of the TiO_2/ZnO heterojunction array, revealing that one-dimensional array structure remained intact after the ALD of ZnO (Figure S1 in Supplementary Information (SI) for low-magnification image). The TiO_2 nanorods were overcoated with thin layer, rendering their lateral surface rough. Energy dispersive X-ray spectroscopy (EDS) analysis in Figure 2(d) confirmed that the rough, thin layer was ZnO, and no other impurities were not found in the TiO_2/ZnO heterojunction array. SEM-EDS mapping analysis also

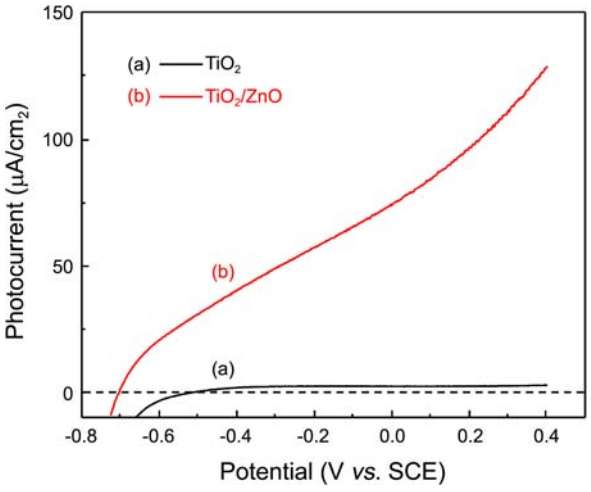

Figure 3. Current-potential plots of (a) TiO_2 and (b) TiO_2/ZnO photoelectrodes (electrolyte: 0.1 M NaOH solution, Pt counter electrode, and excitation: $\lambda > 300$ nm, 100 mW/cm^2).

revealed that the ZnO coating were uniform throughout the entire TiO_2 nanorods (Figure S2 in SI). The thickness of the ZnO layer was examined using a transmission electron microscope (TEM), and it was found to be ~17 nm thick (Figure S3 in SI). Our analysis clearly demonstrates that ALD is a powerful technique for the conformal coating of inorganic thin film and can readily overcome the constraint encountered in the wet-chemical process of ZnO deposition over the hydrophobic TiO_2 nanoarray.

The catalytic activity of the TiO_2 and TiO_2/ZnO nanorod array in photoelectrochemical water splitting cell was compared in Figure 3. The TiO_2 nanorod array generated only small photocurrent even with high bias voltages applied. Upon being coupled with ZnO, however, the TiO_2 array showed *significantly* greater photocurrent, and its photocurrent response to on-off cycles of UV illumination revealed the stability of the photocurrent generation (Figure S4 in SI). This photocurrent gain can be attributed to the enhanced electron-hole separation at the TiO_2/ZnO heterojunction as demonstrated in previous reports.[28-30] This improvement may also result from a complementary effect of electron injection from ZnO to TiO_2 since the electrons can quickly transport through TiO_2 scaffold and thus boost up photocurrent. The combination of two effects for the improved photocurrent cannot be completely excluded either. It is important to note that the onset potential of the TiO_2/ZnO heterojunction was shifted negatively by ~0.18 V in comparison with that of TiO_2. This observation is in parallel with the observation in other heterojunctions such as TiO_2/ZnO, TiO_2/Au, TiO_2/$SrTiO_3$, and WO_3/TiO_2.[22,28,42-44] The onset potential (often known as flat band potential) in general reflects the apparent Fermi level of a semiconductor photoelectrode in equilibrium with a redox couple.[22] The negative shift in flat band potential is therefore indicative of the influence of ZnO on the Fermi level of TiO_2. Coupling TiO_2 with ZnO aids in reducing charge recombination, which results in the accumulation of a larger number of electron in

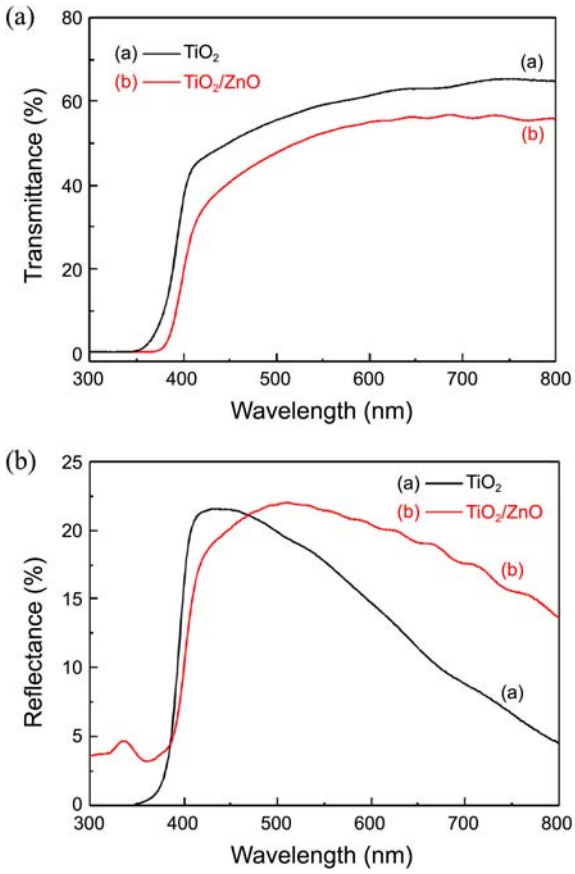

Figure 4. (a) Transmission and (b) reflection spectra of (a) TiO_2 and (b) TiO_2/ZnO heterojunction array.

the TiO_2/ZnO heterojunction. This elevates the Fermi level of the TiO_2/ZnO heterojunction, leading to the increase in internal energy that can be extracted from the photoanode.[45] Therefore, the TiO_2/ZnO heterojunction can relieve its burden to drive water splitting more than TiO_2 (*i.e.*, less overpotential), which appears as the remarkable increase in photocurrent.

The optical behavior of the TiO_2/ZnO heterojunction array was also investigated. Figure 4 shows the transmission and reflection spectra of the TiO_2 and TiO_2/ZnO heterojunction array, respectively. When electromagnetic radiation (*i.e.*, light) is directed on the arrays, the light can be absorbed, transmitted, or scattered. Since ZnO has a wide bandgap (3.2 eV), thus being capable of absorbing only UV light, one could rationally assume that the absorption property of the TiO_2/ZnO heterojunction array would not significantly differ from that of the TiO_2 nanorod array. The transmission spectrum of the TiO_2/ZnO heterojunction array was indeed nearly similar to that of the TiO_2 nanorod array except that the absorption edge is a bit red-shifted. This red shift of the absorption edge is consistent with the previous report, which is ascribed to a subtle change in the bandgap of the TiO_2/ZnO heterojunction.[28] In addition, we noticed that the transmittance of the TiO_2/ZnO heterojunction array decreased a bit over the entire visible light region as opposed to that of the TiO_2 nanorod array. This implies that our TiO_2/ZnO

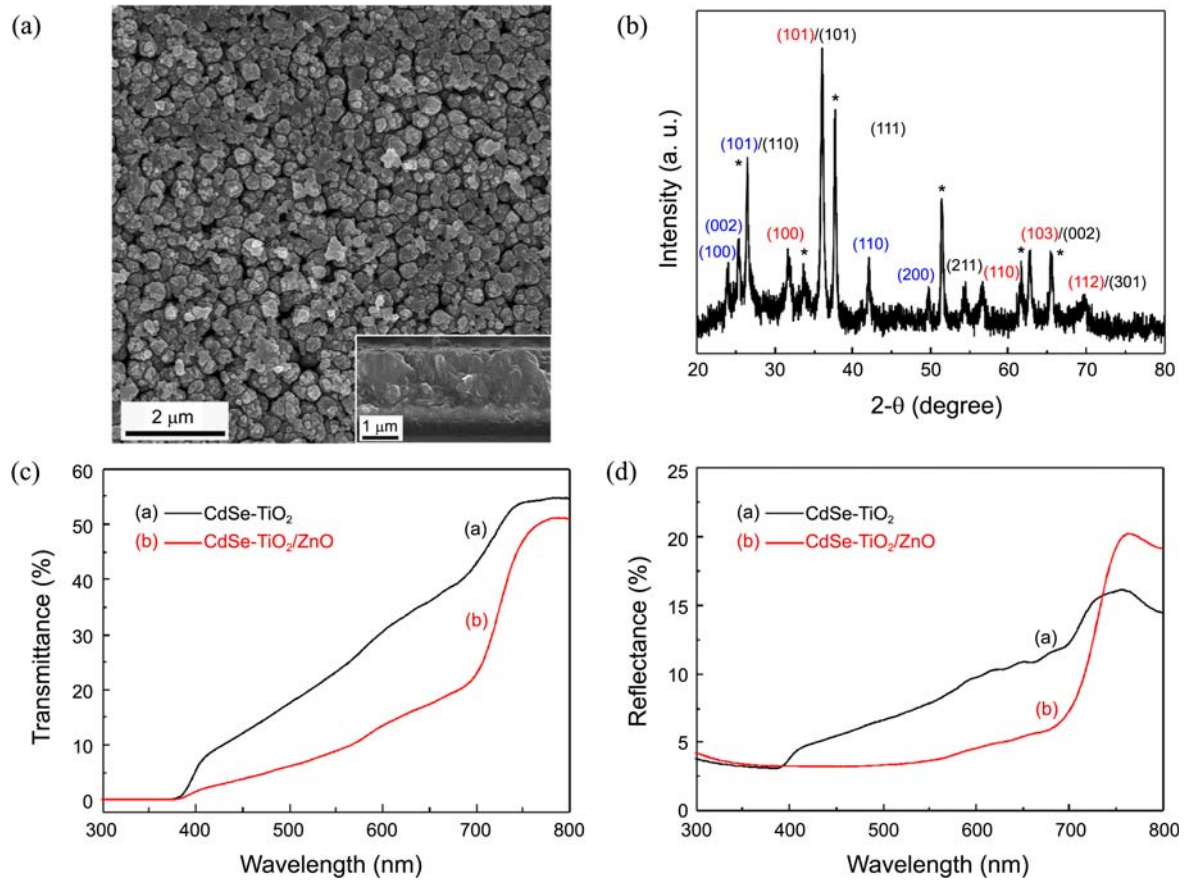

Figure 5. (a) SEM images (inset: cross-section image) and (b) XRD pattern of CdSe-TiO_2/ZnO photoelectrode (peaks from CdSe were labelled in blue); (c) transmission and (d) reflection spectra of (a) CdSe-TiO_2 and (b) CdSe-TiO_2/ZnO photoelectrodes.

heterojunction array possesses a distinct reflection property as compared to the TiO_2 nanorod array. The diffuse reflectance spectrum of the TiO_2/ZnO heterojunction array reveals that it can reflect more light than the TiO_2 counterpart over the entire visible light region, suggesting that light scattering occurs more effectively on the TiO_2/ZnO heterojunction array. This superior light scattering ability could be beneficial for harvesting more visible light if it is coupled with a proper visible light absorbing material.

Our TiO_2/ZnO heterojunction array lends itself well to an oxide substrate for semiconductor-sensitized solar cells because of the excellent scattering property and the superior ability of inner TiO_2 nanorods for fast electron transport demonstrated in our previous report.[17] To prove the usefulness of the TiO_2/ZnO heterojunction array, CdSe was deposited using an electrochemical deposition technique. Not only does CdSe possess a suitable band positions that can form a type-II band alignment, but it can also absorb whole visible light. Figure 5(a) shows the SEM images of the TiO_2/ZnO heterojunction array decorated with CdSe (CdSe-TiO_2/ZnO), revealing that CdSe was uniformly deposited over the entire TiO_2/ZnO heterojunction array. XRD analysis (Figure 5(b)) affirms the deposition of CdSe, and the crystal structure of CdSe was found to be wurtzite. The transmittance of each photoelectrode was inspected, and Figure 5(c) shows that the CdSe-TiO_2/ZnO absorbs more light than the CdSe-TiO_2 throughout the whole visible light region. This overall improvement in absorption results from the significantly decreased optical loss due to the superior scattering effect of the TiO_2/ZnO heterojunction array. The reflectance measurement of each photoelectrode lends support to our hypothesis (Figure 5(d)). In comparison with the CdSe-TiO_2, the CdSe-TiO_2/ZnO reflects less visible light

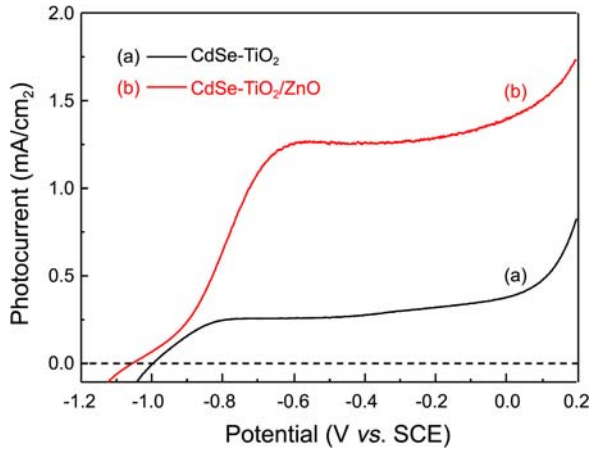

Figure 6. Current-potential plots of (a) CdSe-TiO_2 and (b) CdSe-TiO_2/ZnO photoelectrodes (electrolyte: 0.1 M Na_2S solution, Pt counter electrode, and excitation: AM 1.5 illumination, 57 mW/cm^2).

as the better light scattering in the TiO_2/ZnO heterojunction array enables more photons to be absorbed by CdSe.

Figure 6 compares the photoelectrochemical performance of the CdSe-TiO_2 and of CdSe-TiO_2/ZnO photoelectrodes under visible light illumination (AM 1.5, 57 mW/cm^2). While the electrodeposition of CdSe is not fully optimized at present, this observation clearly proved the usefulness of our TiO_2/ZnO heterojunction array as an oxide substrate. Upon being illuminated, the CdSe-TiO_2/ZnO photoelectrode generated 5-fold greater photocurrent than the CdSe-TiO_2 counterpart. As our study on the optical properties suggests, a significantly greater number of photons were absorbed by CdSe when it was deposited on the TiO_2/ZnO nanorods than on the TiO_2 nanorods. The more photons can generate more electron-hole pairs; therefore, more electrons could be captured by the oxide substrate, leading to greater photocurrent. Along with the contribution from better light absorption, we speculate that the core/shell nanostructure may also play a role in enhancing the performance as we demonstrated earlier that the core/shell nanostructure could impede back-electron transfer from oxide to electrolyte.[46,47] Currently, we are investigating this system using spectroscopic and electrochemical techniques to obtain more insight into recombination characteristics at the interface between the photoelectrode and electrolyte.

Conclusions

One-dimensional semiconductor photoelectrode directly deposited on OTE emerges as a solution that can address several issues associated with thin semiconductor nanoparticulate film. While a recently developed hydrothermal synthesis was successful in growing TiO_2 nanorods on OTE even without a seed layer, the rutile-phase TiO_2 nanorod array was inadequate as a photoanode in photoelectrochemical water-splitting system because of its low conduction band energy level. A core/shell structured TiO_2/ZnO heterojunction that possesses type-II band alignment was fabricated using ALD technique to alleviate such problem in this study. The ALD of ZnO overcomes the synthetic difficulties associated with the hydrophobicity of the TiO_2 nanorod array and allows for conformal ZnO coating over the TiO_2 nanorods. The TiO_2/ZnO heterojunction array was utilized in a photoelectrochemical cell, and we demonstrated that the TiO_2/ZnO heterojunction array was superior to the TiO_2 nanorod array for water oxidation because of significantly improved charge separation and additional electron supply from ZnO to TiO_2. Our TiO_2/ZnO heterojunction array even showed a beneficial optical behavior (better light scattering), which led us to assess its feasibility as an oxide substrate for semiconductor-sensitized solar cell. Our investigation revealed that upon being decorated with CdSe, the TiO_2/ZnO heterojunction array exhibited much higher photocurrent than TiO_2 nanorod array, which is attributed to effective visible light harvesting in the TiO_2/ZnO heterojunction array. We believe that this novel nano-architecture provides a way to develop efficient solar energy conversion systems.

Acknowledgments. This work was supported by the Human Resources Development of the Korea Institute of Energy Technology Evaluation and Planning (KETEP) grant (No. 20104010100620) funded by the Ministry of Knowledge Economy of Korea and by a grant (No. 405-111-004) from Eco-Innovation project funded by the Ministry of Environment of Korea.

Supporting Information Available. SEM image, SEM-EDS mapping analysis, and TEM image of TiO_2/ZnO; Photocurrent responses of TiO_2/ZnO electrode upon on-off cycles of illumination.

References

1. Lewis, N. S.; Nocera, D. G. *Proc. Natl. Acad. Sci. U.S.A.* **2006**, *103*, 15729-15735.
2. Barreca, D.; Carraro, G.; Gombac, V.; Gasparotto, A.; Maccato, C.; Fornasiero, P.; Tondello, E. *Adv. Funct. Mater.* **2011**, *21*, 2611-2623.
3. Maeda, K.; Domen, K. *J. Phys. Chem. Lett.* **2010**, *1*, 2655-2661.
4. Kitano, M.; Hara, M. *J. Mater. Chem.* **2010**, *20*, 627-641.
5. Kudo, A.; Miseki, Y. *Chem. Soc. Rev.* **2009**, *38*, 253-278.
6. Bang, J. H.; Helmich, R. J.; Suslick, K. S. *Adv. Mater.* **2008**, *20*, 2599-2603.
7. Osterloh, F. E. *Chem. Mater.* **2008**, *20*, 35-54.
8. Fujishima, A.; Honda, K. *Nature* **1972**, *238*, 37-38.
9. Chen, X.; Mao, S. S. *Chem. Rev.* **2007**, *107*, 2891-2959.
10. Liu, G.; Wang, L.; Yang, H. G.; Cheng, H.-M.; Lu, G. Q. *J. Mater. Chem.* **2010**, *20*, 831-843.
11. Lee, K.; Kim, D.; Roy, P.; Paramasivam, I.; Birajdar, B. I.; Spiecker, E.; Schmuki, P. *J. Am. Chem. Soc.* **2010**, *132*, 1478-1479.
12. Roy, P.; Das, C.; Lee, K.; Hahn, R.; Ruff, T.; Moll, M.; Schmuki, P. *J. Am. Chem. Soc.* **2011**, *133*, 5629-5631.
13. Yan, J.; Zhou, F. *J. Mater. Chem.* **2011**, *21*, 9406-9418.
14. Shankar, K.; Basham, J. I.; Allam, N. K.; Varghese, O. K.; Mor, G. K.; Feng, X.; Paulose, M.; Seabold, J. A.; Choi, K.-S.; Grimes, C. A. *J. Phys. Chem. C* **2009**, *113*, 6327-6359.
15. Li, S.; Zhang, G.; Guo, D.; Yu, L.; Zhang, W. *J. Phys. Chem. C* **2009**, *113*, 12759-12765.
16. Allam, N. K.; Poncheri, A. J.; El-Sayed, M. A. *ACS Nano* **2011**, *5*, 5056-5066.
17. Bang, J. H.; Kamat, P. V. *Adv. Funct. Mater.* **2010**, *20*, 1970-1976.
18. Wolcott, A.; Smith, W. A.; Kuykendall, T. R.; Zhao, Y.; Zhang, J. Z. *Small* **2009**, *5*, 104-111.
19. Bak, T.; Nowotny, J.; Sucher, N. J.; Wachsman, E. *J. Phys. Chem. C* **2011**, *115*, 15711-15738.
20. Tena-Zaera, R.; Katty, A.; Bastide, S.; Levy-Clement, C. *Chem. Mater.* **2007**, *19*, 1626-1632.
21. Cocivera, M.; Darkowski, A.; Love, B. *J. Electrochem. Soc.* **1984**, *131*, 2514-2517.
22. Zhang, J.; Bang, J. H.; Tang, C.; Kamat, P. V. *ACS Nano* **2010**, *4*, 387-395.
23. Paramasivam, I.; Nah, Y.-C.; Das, C.; Shrestha, N. K.; Schmuki, P. *Chem. Eur. J.* **2010**, *16*, 8993-8997.
24. Lin, Y.; Zhou, S.; Sheehan, S. W.; Wang, D. *J. Am. Chem. Soc.* **2011**, *133*, 2398-2401.
25. Shi, J.; Hara, Y.; Sun, C.; Anderson, M. A.; Wang, X. *Nano Lett.* **2011**, *11*, 3413-3419.
26. Su, J.; Guo, L.; Bao, N.; Grimes, C. A. *Nano Lett.* **2011**, *11*, 1928-1933.
27. McDonald, K. J.; Choi, K.-S. *Chem. Mater.* **2011**, *23*, 4863-4869.
28. Lei, Y.; Zhao, G.; Liu, M.; Zhang, Z.; Tong, X.; Cao, T. *J. Phys. Chem. C* **2009**, *113*, 19067-19076.

29. Chen, D.; Zhang, H.; Hu, S.; Li, J. *J. Phys. Chem. C* **2007**, *112*, 117-122.
30. Shaogui, Y.; Xie, Q.; Xinyong, L.; Yazi, L.; Shuo, C.; Guohua, C. *Phys. Chem. Chem. Phys.* **2004**, *6*, 659-664.
31. Wang, J.; Liu, X.-L.; Yang, A.-L.; Zheng, G.-L.; Yang, S.-Y.; Wei, H.-Y.; Zhu, Q.-S.; Wang, Z.-G. *Appl. Phys. A* **2011**, *103*, 1099-1103.
32. Gerischer, H. *J. Electrochem. Soc.* **1966**, *113*, 1174-1182.
33. Wolcott, A.; Smith, W. A.; Kuykendall, T. R.; Zhao, Y.; Zhang, J. Z. *Adv. Funct. Mater.* **2009**, *19*, 1849-1856.
34. Kostedt; Ismail, A. A.; Mazyck, D. W. *Ind. Eng. Chem. Res.* **2008**, *47*, 1483-1487.
35. Yang, X.; Wolcott, A.; Wang, G.; Sobo, A.; Fitzmorris, R. C.; Qian, F.; Zhang, J. Z.; Li, Y. *Nano Lett.* **2009**, *9*, 2331-2336.
36. Steinmiller, E. M. P.; Choi, K.-S. *Proc. Natl. Acad. Sci. U.S.A.* **2009**, *106*, 20633-20636.
37. Paulauskas, I. E.; Katz, J. E.; Jellison, G. E., Jr.; Lewis, N. S.; Boatner, L. A. *Thin Solid Films* **2008**, *516*, 8175-8178.
38. Feng, X.; Zhai, J.; Jiang, L. *Angew. Chem. Int. Ed.* **2005**, *44*, 5115-5118.
39. Gu, F.; Gai, L.; Shao, W.; Li, C.; Schmidt-Mende, L. *Chem. Commun.* **2011**, *47*, 8400-8402.
40. George, S. M. *Chem. Rev.* **2009**, *110*, 111-131.
41. Bang, J. H.; Suslick, K. S. *Adv. Mater.* **2009**, *21*, 3186-3190.
42. Subramanian, V.; Wolf, E. E.; Kamat, P. V. *J. Am. Chem. Soc.* **2004**, *126*, 4943-4950.
43. Jakob, M.; Levanon, H.; Kamat, P. V. *Nano Lett.* **2003**, *3*, 353-358.
44. Smith, W.; Wolcott, A.; Fitzmorris, R. C.; Zhang, J. Z.; Zhao, Y. *J. Mater. Chem.* **2011**, *21*, 10792-10800.
45. Walter, M. G.; Warren, E. L.; McKone, J. R.; Boettcher, S. W.; Mi, Q.; Santori, E. A.; Lewis, N. S. *Chem. Rev.* **2010**, *110*, 6446-6473.
46. Zhang, J.; Tang, C.; Bang, J. H. *Electrochem. Commun.* **2010**, *12*, 1124-1128.
47. Law, M.; Greene, L. E.; Radenovic, A.; Kuykendall, T.; Liphardt, J.; Yang, P. *J. Phys. Chem. B* **2006**, *110*, 22652-22663.